

Article

Assessing Water and Nutrient Long-Term Dynamics and Loads in the Enxoé Temporary River Basin (Southeast Portugal)

David Brito ^{1,*}, Ramiro Neves ¹, Maria A. Branco ², Ângela Prazeres ², Sara Rodrigues ², Maria C. Gonçalves ² and Tiago B. Ramos ¹

¹ Centro de Ciência e Tecnologia do Ambiente e do Mar (MARETEC), Instituto Superior Técnico, Universidade de Lisboa, Av. Rovisco Pais, 1, 1049-001 Lisboa, Portugal; ramiro.neves@tecnico.ulisboa.pt (R.N.); tiagobramos@tecnico.ulisboa.pt (T.B.R.)

² Instituto Nacional de Investigação Agrária e Veterinária (INIAV), Quinta do Marquês, Av. República, 2784-505 Oeiras, Portugal; amelia.castelobranco@iniav.pt (M.A.B.); acoprazers@hotmail.pt (Â.P.); sara.rodrigues@ua.pt (S.R.); maria.goncalves@iniav.pt (M.C.G.)

* Correspondence: odavidbrito@gmail.com; Tel.: +35-121-841-9428

Received: 25 January 2019; Accepted: 15 February 2019; Published: 19 February 2019



Abstract: The Enxoé reservoir has been exhibiting frequent high chlorophyll-a concentrations (reaching a geometric mean six times the national limit for eutrophication of $10 \mu\text{g L}^{-1}$) since 2000, and represents the reservoir with the highest eutrophic state in Portugal. Toxic algal blooms have also been observed, which pose serious challenges to water managers, as the reservoir is used for potable water production. In an effort to contribute to the reduction of the reservoir trophic state, the watershed inputs (monthly flows, sediment, nitrogen (N) and phosphorus (P) loads) were characterized with the Soil Water Assessment Tool (SWAT). Field data were collected in the ungauged watershed during 2010 and 2011. Model results were then used to characterize the long-term watershed dynamics in terms of water and nutrients. SWAT estimates of the simulated flow, and the sediment and nutrient loads were in good agreement with field data (R^2 between 0.42–0.78; Nash-Sutcliffe efficiencies between 0.19–0.75). The Enxoé River was characterized by a temporary flushy regime where high concentrations were transported in short time periods. As a result, nutrient loads delivered to the Enxoé reservoir were estimated to be $18 \text{ tonN year}^{-1}$ and $0.7 \text{ tonP year}^{-1}$ (30 years' simulation), reaching the reservoir mainly by runoff. These results were consistent with the gentle slopes, extensive agricultural activities, and low urban pressure observed in Enxoé. The magnitude of the nutrient exports suggests that the reservoir eutrophication may also be linked to the reservoir geometry (average depth of 5 m), which provides high light availability to the bottom sediments. Thus, SWAT results were integrated into a reservoir model to depict the origin of the Enxoé trophic state and test management scenarios that may reduce it.

Keywords: Enxoé; eutrophic reservoir; nutrients; watershed modeling; SWAT model

1. Introduction

Enxoé is a temporary river located in the Alentejo region, in southeast Portugal, and is one of the tributaries of the Guadiana river. The Enxoé catchment is limited downstream by a reservoir built in 1998, which has been exhibiting the highest eutrophic state in the country ever since [1,2]. Since 2000, the reservoir has had frequent chlorophyll-a concentrations higher than $50 \mu\text{g L}^{-1}$. The geometric average of the surface chlorophyll-a concentration measured from April to September between 1998–2009 was approximately $60 \mu\text{g L}^{-1}$ [3], whereas the national limit for eutrophication is $10 \mu\text{g L}^{-1}$. Moreover, toxic cyanobacteria blooms occurred [4,5] and interrupted the water distribution to the local

population. This constitutes a serious problem for water management, with the constant reservoir eutrophication, particularly the presence of toxic algae in a reservoir used for water production, calling for improved management plans in the scope of the Water Framework Directive.

Cyanobacteria algae dominance is usually described by two main processes; the capability of consuming N_2 dissolved in water [6–8], and the capability of maintaining growth even under conditions of low light availability [7]. The nitrogen fixation characteristics of some types of cyanobacteria allows them to be independent of the availability of inorganic forms of nitrogen (e.g., ammonia, nitrate). However, under conditions of nitrogen limitation, cyanobacteria have also the potential to generate blooms if phosphorus is available [7].

Such cyanobacterial response to phosphorus availability may have occurred in the Enxoé reservoir after 2002 when these species became dominant [4,9]. 2000/2001 was a wet hydrologic year, and the winter floods transported adsorbed material into the reservoir. The first blooms consumed the available inorganic material while organic matter deposited. The accumulation of organic matter at the bottom of the reservoir and the corresponding increase in mineralization may have depleted the oxygen near the bottom (where mineralization is more intense). Thus, under these anoxic conditions, phosphorus may have been released from the adsorbed phase to the water column and fueled blooms. These processes were noted by Coelho et al. [9] as the probable drivers for algal bloom in Enxoé, and also for cyanobacterial dominance. Those authors further linked the cyanobacteria blooms in the reservoir to the input loads from the watershed, and considered that such blooms could be associated with phosphorus input. Usually, phosphorus is adsorbed onto fine soil particles and transported throughout the catchment associated with water erosion. Phosphorus feeding from the watershed may have fueled the process, which consists of both a fast and a delayed response in the reservoir (initial blooms arise from the consumption of input dissolved nutrients, while later blooms are attributable to sediment sources, e.g., mineralization and desorption under anoxic conditions). The same need for understanding the role of erosion and phosphorus inputs in Enxoé reservoir blooms was also stated by Ramos et al. [10,11].

The understanding of the Enxoé trophic state must ultimately integrate the watershed and the reservoir in order to determine the impact in the reservoir of management responses in the watershed (e.g., changes in agricultural practices, erosion control). This includes coupling a watershed model and a reservoir model (integrating the available data) to determine the best-suited management strategies (in the watershed and/or reservoir) to reduce the reservoir trophic status. However, there is first the need for understanding the watershed dynamics and quantifying nutrient feeding into the Enxoé reservoir.

The SWAT model [12] was here used for watershed characterization of the long-term fluxes to the reservoir. This model has been widely applied to a range of watershed sizes and configurations to simulate flow and nutrient export on daily, monthly and annual scales [13,14]. Examples of such implementation in small-sized watersheds with similar land uses as Enxoé can be found in Geza and McCray [15], and Green and van Griensven [16], both in the USA; Yevenes and Mannaerts [17] application for quantifying nitrogen export in a Portuguese catchment; Dechmi et al. [18] and Panagopoulos et al. [19] in other semi-arid Mediterranean watersheds in Spain and Greece, respectively; and Debele et al. [20] who also successfully linked SWAT to the reservoir model CE-QUAL-W2 for water quality management.

The objectives of this study were thus to understand the water and nutrient long-term dynamics in the Enxoé catchment using the SWAT model, and to quantify nutrient loads to the Enxoé reservoir. As the Enxoé basin was ungauged, field data were first collected between 2010 and 2011 in order to calibrate the model. This study is the first of a series of modeling studies aimed at improving water management plans in the Enxoé basin [21–23].

2. Materials and Methods

2.1. Study Area

Enxoé is a 60 km² catchment located in southeast Portugal, in the left margin of the Guadiana River (Figure 1). The river has a bed length of approximately 9 km from its headwaters to the reservoir. The reservoir (37°59′38.12″ N; 7°27′54.78″ W) limits the catchment downstream, and has a total volume of 10.4 hm³, a surface area of approximately 2 km², and an average depth of 5 m.

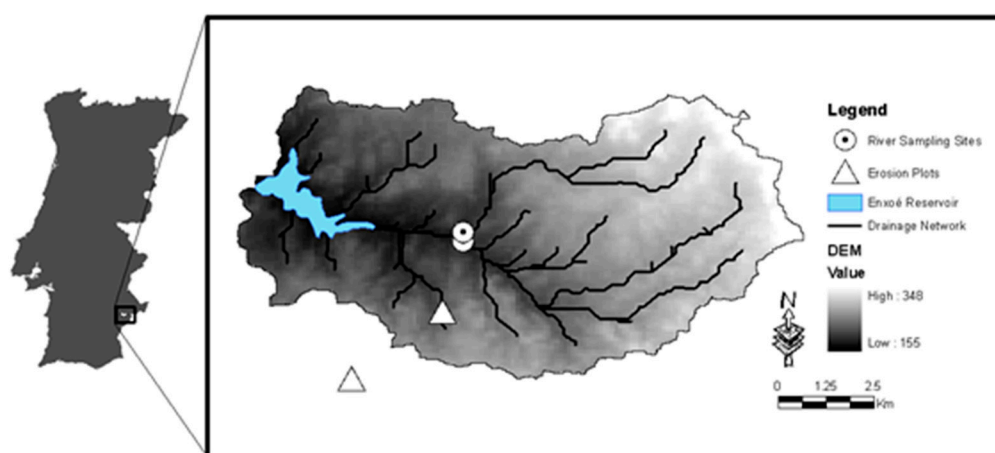


Figure 1. Location of the Enxoé catchment and monitoring stations.

The climate in the region is dry sub-humid to semi-arid. The annual average precipitation is 500 mm, irregularly distributed throughout the year (80% of the annual precipitation is concentrated between October and April). The slopes are gentle, with the river showing an average slope of approximately 2%, while the catchment has an average slope of 5–6%. The soils in Enxoé originate mainly from granite and limestone (each with approximately 30% of the total area) and schist (with approximately 10% of the total area). The land is mainly used for growing olive trees, agro-forestry of holm-oaks (“montado”), and annual rainfed crops (wheat, oats, and sunflower), each covering approximately 30% of the total area (Figure 2; Table 1). Extensive livestock production is the most important animal-farming activity in the catchment [24]. The catchment has a population of 1000 inhabitants, mainly concentrated in Vale de Vargo (Figure 2). The respective waste water treatment plant discharges outside the watershed since 2006 as a protective measure to the Enxoé reservoir. The reservoir currently supplies the villages of Mértola and Serpa (25,000 inhabitants).

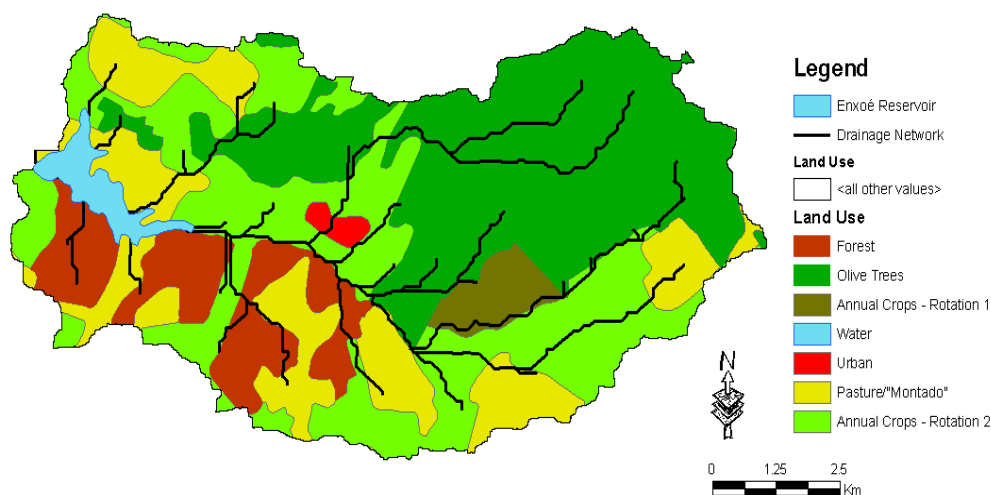


Figure 2. Land use distribution map [25].

Table 1. Enxoé land use [25].

Land Use	Area	
	(km ²)	(%)
Olive trees	21	35%
Annual crops—Rotation 2	18	30%
Agro-forestry of holm-oaks (Pasture/“Montado”)	11	19%
Agro-forestry of holm oaks (Forest/ “Montado”)	7	11%
Annual crops—Rotation 1	2	3%
Water	1	2%
Urban area	<1	<1%
Total	61	100%

2.2. SWAT Model Description

SWAT is a basin-scale, distributed, and continuous-time model [12] that includes the main hydrological and nutrient processes occurring in an extensive Mediterranean catchment like Enxoé (e.g., flow temporality, crops, agricultural practices). The SWAT model divides the watershed into sub-basins and hydrological response units (HRU) that are homogeneous in terms of soil, land use, and slope (the basic computation units). The soil domain may be divided into vertical layers.

The hydrological cycle is based on the computation of the soil water balance equation, as follows [12]:

$$W_t = SW_0 + \sum_{i=1}^t (R_{\text{day}} - Q_{\text{surf}} - E_a - Q_{\text{perc}} - Q_{\text{gw}}) \quad (1)$$

where SW_t and SW_0 are the final and initial soil water contents (mm), respectively, t is the time (days), R_{day} is the precipitation (mm), Q_{surf} is the surface runoff (mm), E_a is the actual evapotranspiration (mm), Q_{perc} is the percolation (mm), and Q_{gw} is the return flow (mm), all related to day i . The model computes evaporation from soils and plants separately as described by Ritchie [26]. Potential soil water evaporation is predicted as a function of potential evapotranspiration (PET) and leaf area index (LAI), whereas actual soil water evaporation is predicted by using exponential functions of water content and soil depth. Plant transpiration is predicted as a linear function of PET and LAI. In this study, PET was computed with the Penman-Monteith method [27], which requires daily data on solar radiation, wind speed, air temperature, and relative humidity. Q_{perc} is estimated from the soil water content above field capacity, while Q_{gw} is computed by combining a storage routing technique and a crack-flow model [12]. Of particular interest to this study is the estimation of surface runoff (Q_{surf}) which is computed with the modified curve number (CN) method [28], as follows:

$$Q_{\text{surf}} = \frac{(R_{\text{day}} - I_a)^2}{(R_{\text{day}} - I_a + S)} \quad (2)$$

where I_a is the initial abstractions which include surface storage, interception, and infiltration prior to runoff (mm), and S a retention parameter which varies with the soil type, land use, land management, slope, and soil water content. On the other hand, the subsurface flow (Q_{lat}) is simulated using a kinematic storage method dependent of the surface slope and soil water content [12].

Soil erosion in SWAT is computed from rainfall and surface runoff with the Modified Universal Soil Loss Equation (MUSLE) [29], which is a modified version of the Universal Soil Loss Equation (USLE) developed by Wischmeier and Smith [30]. In MUSLE, the rainfall energy factor is replaced with a runoff factor, as follows:

$$\text{sed} = 11.8 \left(Q_{\text{surf}} q_{\text{peak}} \text{area}_{\text{HRU}} \right)^{0.56} K_{\text{USLE}} C_{\text{USLE}} P_{\text{USLE}} L_{\text{USLE}} C_{\text{FRG}} \quad (3)$$

where sed is the sediment yield on a given day (ton), q_{peak} is the peak runoff rate ($m^3 s^{-1}$), $area_{HRU}$ is the area of the HRU (ha), K_{USLE} is the USLE soil erodibility factor, C_{USLE} is the USLE cover and management factor, P_{USLE} is the USLE support practice factor, LS_{USLE} is the USLE topographic factor, and $CFRG$ is the coarse fragment factor. The SWAT model peak runoff rates are computed by a modified rational formula with the following form [12]:

$$q_{peak} = \frac{\alpha_{tc} \times Q_{surf} \times area_{HRU}}{3.6 \times t_c} \quad (4)$$

$$\alpha_{tc} = 1 - \exp[2 \times t_c \times \ln(1 - \alpha_{0.5})] \quad (5)$$

where α_{tc} is the fraction of the daily rainfall that occurs during the time of concentration (-), t_c is the concentration time (h), and $\alpha_{0.5}$ is the fraction of the daily rain at the highest half hour intensity (-).

The nutrient component of the SWAT model includes inputs from agriculture, transport with runoff and groundwater, consumption by plants, and mineralization processes occurring in the soil [12]. SWAT considers six different pools of phosphorus (P) in the soil. Three pools are inorganic forms of P while the other three pools are organic forms of P. Fresh organic P is associated with crop residue and microbial biomass. Active and stable organic P pools are associated with the soil humus. The organic P associated with humus is portioned into two pools to account for the variation in availability of humic substances to mineralization. Soil inorganic P is divided into solution, active, and stable pools. The solution pool is in rapid equilibrium (several days or weeks) with the active pool. The active pool is in slow equilibrium with the stable pool [12].

P is mainly removed from the soil by plant uptake and erosion. In the latter case, SWAT considers the amount of organic and mineral P transported with sediment to the stream with a loading function developed by McElroy et al. [31] and later modified by Williams and Hann [32], as follows:

$$sedP_{surf} = 0.001 conc_{sedP} \frac{sed}{area_{HRU}} \epsilon_{P:sed} \quad (6)$$

where $sedP_{surf}$ is the amount of P transported with sediment to the main channel in surface runoff ($kg ha^{-1}$), $\epsilon_{P:sed}$ is the P enrichment ratio, sed is the sediment yield (tons), $area_{HRU}$ is the HRU area (ha) and $conc_{sedP}$ is the concentration of P attached to sediment in the top 10 mm ($g ton^{-1}$), which is computed from the amount of P in the different pools, as:

$$conc_{sedP} = 100 \frac{(\min P_{act,surf} + \min P_{sta,surf} + orgP_{hum,surf} + orgP_{frsh,surf})}{\rho_b depth_{surf}} \quad (7)$$

where $\min P_{act,surf}$ is the amount of P in the active mineral pool ($kg ha^{-1}$), $\min P_{sta,surf}$ is the amount of P in the stable mineral pool ($kg ha^{-1}$), $orgP_{hum,surf}$ is the amount of P in humic organic pool ($kg ha^{-1}$), $orgP_{frsh,surf}$ is the amount of P in the fresh organic pool ($kg ha^{-1}$), all related to top 10 mm ($depth_{surf}$), and ρ_b is the bulk density of the top soil layer ($ton m^{-3}$).

Nitrogen (N) is extremely reactive and exists in a number of dynamic forms. It may be added to the soil in the form of fertilizer, manure or residue application, bacteriological fixation, and rain. In SWAT, there are five different pools of N in the soil. Two of the pools are inorganic forms of N, while the other three pools are organic forms of N. N transport occurs mainly in the nitrate and organic N forms.

Nitrate may be transported with surface runoff, lateral flow or percolation, using the following generic formula [8]:

$$NO_3 = \beta_{NO_3} conc_{NO_3, mobile} Q_x \quad (8)$$

where NO_3 is the nitrate removed by each of the physical transport mechanisms here considered (i.e., surface runoff, lateral flow, percolation) ($kg ha^{-1}$), β_{NO_3} is concentration of nitrate in the mobile water for the top 10 mm of soil ($kg ha^{-1}$) (only considered for surface runoff and subsurface lateral flow

in the top layer), and Q_x is the physical transport mechanism considered (Q_{surf} , Q_{lat} , Q_{perc}). Nitrate entering the shallow aquifer from the soil profile through percolation (leaching) may remain in the aquifer, be moved with groundwater flow into the main channel, be transported out of the shallow aquifer with water moving into the soil zone in response to water deficiencies or be moved with recharge to the deep aquifer.

On the other hand, organic N is mainly transported with sediment to the stream, similarly to P transport. The same approach developed by McElroy et al. [31] and William and Hann [32] is applied to separate runoff events. The estimation of the daily organic N runoff losses are based on the sediment yield, the N enrichment ratio, and the concentration of N in the topsoil layer, which is dependent of the amount of organic N in the fresh, stable, and active pools [12].

2.3. Model Setup and Calibration

2.3.1. Model Implementation

The SWAT model [12] was used to estimate the long-term water and nutrient dynamics in the Enxoé catchment, and to quantify the nutrient loads to the Enxoé reservoir. Data were introduced in the model interface AVSWAT for ArcView®, and the model was run using the SWAT 2005 executable version. The model was first calibrated against field data, and then results were extrapolated to the basin scale.

Table 2 describes the digital terrain model (DTM), and the land use, soil texture, and weather data used in SWAT. The land use map with SWAT classification is presented in Figure 2, where, as stated previously, olive trees (orchards), agro-forestry of holm-oaks, and annual rainfed crops each represent approximately 30% of the total area (Table 1). The land use map was obtained from Corine 2000 [25], which was first compared with aerial pictures from 2006 and local observations for consistency.

Information about annual agricultural practices (crop rotations and fertilization) was obtained from questionnaires given to farmers. Annual rainfed crops included rotation between wheat and oats (crops rotation 2), and rotation between sunflowers, wheat, and oats (crops rotation 1) (Figure 2). The annual input fertilization loads were estimated to range from 18–80 kgN ha⁻¹ year⁻¹, and approximately 20 kgP ha⁻¹ year⁻¹ (Table 3). The animal nutrient production was obtained from the 1999 national census data [24] (Table 4). Animal loads were distributed homogeneously in the agro-forestry of holm-oaks (sheep and cattle) and olive trees (sheep) sites. The annual animal loads were estimated to range from 6–30 kgN ha⁻¹ year⁻¹ and 1–4 kgP ha⁻¹ year⁻¹. Annual input fertilization and animal loads can be considered low, which is justified by the fact that agriculture and pasturing in the region are extensive.

The Enxoé catchment was ungauged, which partially constrained model calibration/validation due to data limitation. Thus, the model predictions of the inflow to the reservoir were calibrated through a reservoir balance computation using volume, discharge, precipitation, and evaporation data for the period between January 2006 and August 2009, when all the components were available. On the other hand, SWAT nutrient dynamics was calibrated using data collected in the two main tributaries flowing to the Enxoé reservoir (Figure 1) between 2010 and 2011; both monitoring stations were found to have similar concentrations, trends, and values. The river data were collected on a weekly basis (with three samples collected each time) during autumn, winter, spring, and summer, when water existed (temporary river). The parameters evaluated in the laboratory were the electrical conductivity, pH, P, nitrate, and suspended solids. No extensive validation of model simulations was possible due to the data limitations referred to above.

Table 2. Data used for SWAT model implementation.

Data Type	Description	Origin	Resolution	Period	Frequency
DTM	SRTM Digital Elevation	NASA	90 m	-	-
Land Use	Corine Land Cover 2000	EEA	1:100,000	1999–2002	-
Soil Texture	European Soil database	JRC, EU	1:100,000	1996	-
Precipitation	Daily input	Valada and Sobral da Adiça stations, National Water Institute [33]	-	1980–2011	Daily
Other weather data	Temperature, relative humidity, solar radiation, and wind speed monthly averages for weather generator (1980–2000) and daily data (2000–2011)	Serpa station, National Meteorology Institute, and Valada, Sobral da Adiça and Monte da Torre stations, National Water Institute [33]	-	Variant for monthly averages and 2000–2011 for daily data	Monthly averages and daily data after 2000

Table 3. Enxoé agricultural practices (information collected by questioning farmers).

Agricultural Practice	Crop			
	Wheat and Barley	Oats	Sunflower	Olive Trees
Planting	November	October	April	-
Fertilization	November (20 kgN ha ⁻¹) November (18 kgP ha ⁻¹) January (50 kgN ha ⁻¹) February (20 kgN ha ⁻¹)	March (40–80 kgN ha ⁻¹)	April (22 kgP ha ⁻¹)	April to July (24–60 kgN ha ⁻¹)
Harvest	June	June	September	-

Table 4. Number of animals in the Enxoé watershed [24], and annual associated loads [34].

Type	Number	Annual Load	
		Nitrogen (tonN year ⁻¹)	Phosphorus (tonP year ⁻¹)
cattle	602	34	5
sheep	4365	78	13

SWAT performance was further assessed by qualitatively comparing model predictions with erosion data measured in plots (60–900 m²) installed in two of the main land uses (olive trees and agro-forestry of holm-oaks) between 2010 and 2011 (Figure 1). One erosion plot was located outside the catchment due to logistical reasons, but in an area with the same characteristics in terms of land use, soils and slopes as in Enxoé. The runoff volume and concentrations were sampled in the erosion plots in weekly to monthly basis or after heavy rain events. Table 5 summarizes the data used for calibrating/validating flow and water quality in the Enxoé catchment.

Table 5. Description of the data used for SWAT model calibration.

Data Type	Station	Origin	Period	Frequency
Reservoir Inflow:				
Reservoir Discharges	Enxoé Reservoir (26M/01A)	National Water Institute [33]	2005–2009	Monthly
Precipitation	Herdade da Valada (26M/01C), Sobral Adiça (25N/01UG)	National Water Institute [33]	1980–2011	Daily
Evaporation	Herdade da Valada (26M/01C), Monte da Torre	National Water Institute [33]	2001–2011	Daily
Erosion:				
Erosion rates	Two plots in two main land uses. Volume and solids concentrations collected	Measured	2010–2011	Weekly to monthly
Water quality in river:				
Nutrient	Two stations in the two main tributaries	Measured	2010–2011	Weekly to monthly

2.3.2. Calibration Procedure

SWAT calibration procedure involved modifying specific parameters until deviations between model predictions and observations were minimized. The SWAT model sensitivity analysis for discharge revealed that the most important parameters that impacted the results were the moisture condition II curve number (CN2), the threshold water level in shallow aquifer for base flow (Gwqmn), the soil evaporation compensation coefficient (ESCO), and the available water capacity (SOL_AWC) [12]. However, the main differences between the hydrograph produced by using the default parameters available in the SWAT model and the real hydrographs measured in small-sized watersheds without known aquifer interactions in southern Portugal is that the SWAT model creates longer baseflows that last for months after rain events while the peaks are usually lower. These differences occur because the delay time for aquifer recharge (GW_DELAY) and the baseflow recession constant (ALPHA_BF) parameters, which control the travel timing of water between the soil and the aquifer and between the aquifer and the river, are unadjusted for small, temporary river watersheds in which travel times are small and hydrographs have a fast rise and fall correlated to rain events [10]. Thus, in Enxoé, the calibration procedure for hydrology consisted of changing the parameters GW_DELAY and ALPHA_BF as presented in Table 6. The values chosen were the same as those obtained via other SWAT projects in the same area (Alentejo) that compared well the daily flow available and were also of the same order as those used in studies conducted in similar temporary rivers located in arid or semi-arid areas, such as the Meca River, Spain [35], and the Gajwel watershed, India [36].

In terms of water quality, the river stream parameters (Table 6) were adjusted by trial and error to represent the behavior observed in the field data. Although SWAT initial results of total N and total P were satisfactory when compared to field data, the first simulations exhibited overpredictions of organic N, ammonia and inorganic P, and underpredictions of nitrate concentrations, which drove the changes in the rates for mineralization between the organic and inorganic species described in Table 6. In addition, in the first simulations, nitrate and orthophosphate concentrations appeared to be associated only with rain events, which then decreased to almost zero after an event while the respective field data concentrations remained higher throughout.

SWAT uses a QUAL-2E [37] formulation for the river quality, in which P deposition is disconnected from the suspended sediment deposition, and deposition and release are not linked through a sediment

state variable accounting for these fluxes. However, to maintain mass conservation, the results presented were verified so that the average annual deposition loads were higher than the release loads to assure consistency in the selected parameters.

Table 6. Calibrated parameters used in SWAT simulations.

Parameter Description	SWAT Name	SWAT File	Default Value	Calibrated Value
Hydrodynamic:				
Groundwater delay (days)	GW_DELAY	.gw	31	3
Base flow recession alpha factor (days)	ALPHA_BF	.gw	0.048	1
Water Quality:				
Linear parameter for calculating the maximum amount of sediment that can be reentrained during channel sediment routing	SPCON	.bsn	0.0001	0.00005
Organic phosphorus settling rate in the reach at 20 °C (day ⁻¹)	RS5	.swq	0.05	0.35
Benthic (sediment) source rate for dissolved phosphorus in the reach at 20 °C (mg dissolved P m ⁻² .day ⁻¹)	RS2	.swq	0.05	0.5
Benthic source rate for NH ₄ -N in the reach at 20 °C (mg NH ₄ -N m ⁻² .day ⁻¹)	RS3	.swq	0.5	10
Rate constant for hydrolysis of organic N to NH ₄ in the reach at 20 °C (day ⁻¹)	BC3	.swq	0.21	0.25
Rate constant for biological oxidation of NH ₄ to NO ₂ in the reach at 20 °C (day ⁻¹)	BC1	.swq	0.55	2.0
Rate constant for biological oxidation of NO ₂ to NO ₃ in the reach at 20 °C (day ⁻¹)	BC2	.swq	1.1	3.0
Rate constant for mineralization of organic P to dissolved P in the reach at 20 °C (day ⁻¹)	BC4	.swq	0.35	0.01

2.3.3. Statistical Analysis

The model fit to measured data was assessed by comparing field measured data with SWAT simulated values using various qualitative and quantitative measures of the uncertainty. Graphical analyses, such as time-series plots, were used to identify the general trends, potential sources of errors, and differences between the measured and predicted values. The performance of the model was further evaluated using the coefficient of determination (R^2), the root mean squared error (RMSE), and the Nash–Sutcliffe model efficiency (NSE) [38]. R^2 values close to 1 indicate that the model explains well the variance of observations. RMSE values close to zero indicate small errors of estimate and good model predictions. NSE values between 0.0 and 1.0 are generally viewed as acceptable levels of performance, whereas values <0.0 indicate that the mean observed value is a better predictor than the simulated value, corresponding to unacceptable performance [39].

2.3.4. The Long-Term Dynamics of the Enxoé Catchment

After the model calibration, the SWAT model was used to extrapolate results to the long-term in order to better understand the catchment behavior in terms of water and nutrient dynamics. Hence, the water and nutrient balance was computed for a thirty-year period (1980–2010) to account for climate variability. The same data presented in Table 2 was used for the long-term study. Weather data was collected from the meteorological stations of the National Institute of Water [33] located in the vicinity of the Enxoé catchment (Herdade da Valada, Sobral da Adiça, Monte da Torre stations). The same calibrated parameters defined in Table 6 were naturally used in the long-term analysis.

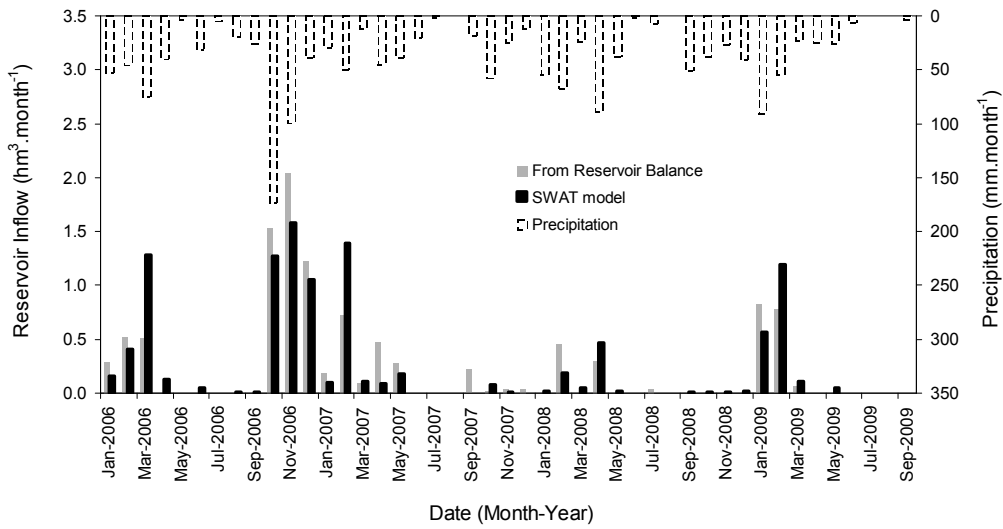
3. Results and Discussion

3.1. Model Results Versus Field Data

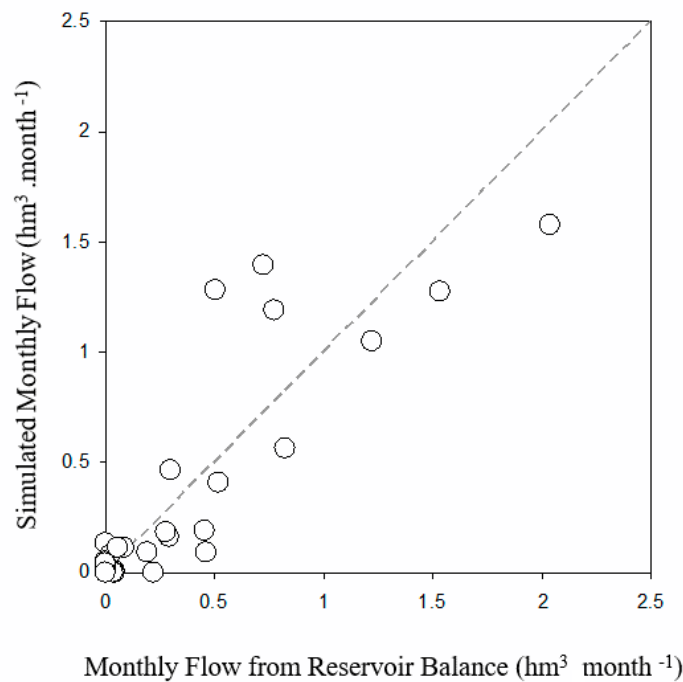
The comparison between the SWAT model and the field data was made with respect to: i) Water inflow to the reservoir, and ii) nutrient loads in the river.

3.1.1. Reservoir Inflow

Figure 3 shows the comparison between monthly flows computed from the reservoir balance and SWAT predictions for 2006–2009. The respective goodness-of-fit tests are presented in Table 7. Both SWAT predictions and the estimates from the reservoir balance exhibited the same trends (higher reservoir inflows in winter as a response to precipitation and a very low or zero inflow in the summer in the absence of rain). The value of R^2 was high (0.78), showing that the model was able to explain the variability of observed data. The error of the estimate was quite small, with RMSE values reaching $0.21 \text{ hm}^3 \text{ month}^{-1}$. The NSE value was also very high (0.77), thus indicating that the mean square error was much smaller than the measured data variance.



(a)



(b)

Figure 3. Comparison between measured (from the reservoir balance) and simulated (SWAT) monthly inflows to the Enxoé reservoir (a); and scatterplot of the measured versus simulated monthly inflow values (b) between 2006–2009.

Table 7. Summary of the comparison of the SWAT model results to the collected data in the Enxoé watershed.

Parameter	Period	Data Average	Model Average	RMSE	R ²	Nash-Sutcliffe Model Efficiency
Flow:						
Monthly Reservoir Inflow	1996–2009	0.24 hm ³ month ⁻¹	0.24 hm ³ month ⁻¹	0.21 hm ³ month ⁻¹	0.78	0.77
Slope Erosion:						
Annual erosion rates	2010–2011	0.1–0.2 ton ha ⁻¹	0.35 ton ha ⁻¹	-	-	-
River Water quality:						
Monthly Total N Load	2010–2011	0.62 tonN month ⁻¹	0.50 tonN month ⁻¹	0.46 tonN month ⁻¹	0.69	0.65
Monthly Total Suspended Solids Load	2010–2011	1.86 tonTSS month ⁻¹	1.80 tonTSS month ⁻¹	2.23 tonTSS month ⁻¹	0.42	0.19
Monthly Total P Load	2010–2011	0.034 tonP month ⁻¹	0.030 tonP month ⁻¹	0.025 tonP month ⁻¹	0.63	0.62

These results are comparable to those reported by Fohrer [40] in two watersheds in Hesse, Germany (R² of 0.71–0.92); Geza and McCray [15] in Turkey Creek (126 km²), Denver, USA (R² of 0.62–0.74; NSE of 0.61–0.70); and Green and van Griensven [16] in different small watersheds in Texas, USA (R² from 0.60–0.96; NSE from 0.59–0.95). In the Mediterranean region, Dechmi et al. [18] obtained high R² and NSE values of 0.90 in the Del Reguero River watershed (20 km²) in northern Spain, while Panagopoulos et al. [19] found R² values of 0.86–0.92 and NSE values of 0.51–0.68 in the Arachthos catchment (2000 km²), in western Greece. Thus, in terms of the monthly flow, the results obtained in Enxoé fall in between the results of other studies, showing that the SWAT model was able to represent the inflow to the reservoir on a monthly scale.

3.1.2. River Sediment and Nutrient Loads

Loads can give insights about the pressures that the Enxoé reservoir is subjected to, and are dependent on the catchment hydrology. Sediment and nutrient loads were estimated using SWAT daily flow predictions for the monitored period (2010–2011), using the same calibrated parameters for assessing the inflows to the reservoir on a monthly scale (Table 6). During 2010–2011, the Enxoé River, as temporary, exhibited no flow or ephemeral conditions from June to October (Figure 4). The first rain events (October/November) generated flow peaks that were quickly reduced as the soil was not fully saturated and the groundwater flow was greatly diminished. From December/January to March, the response to rain events still existed. Because the soil was saturated, baseflows were maintained for longer periods but still fell quickly, especially during months with less rain (January and February 2011). This temporality and flushy flow regime strongly influenced loads to the Enxoé reservoir, particularly as these conditions created long periods of low waters with increased retention times that had consequences for the river water quality and promoted in-stream processes, as observed in a similar-sized catchment by Lillebø et al. [41].

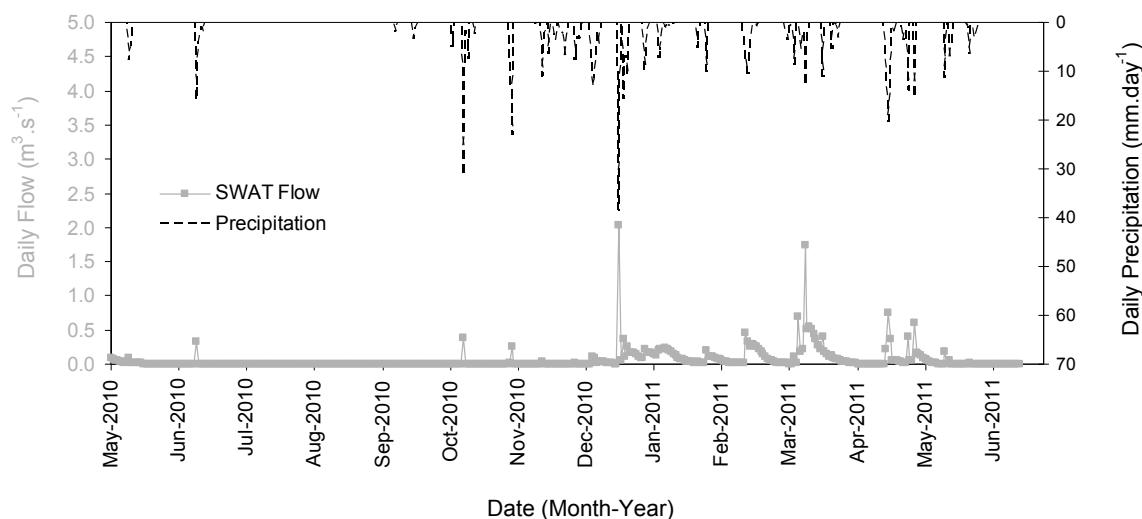


Figure 4. SWAT estimate of the Enxoé river flow during 2010–2011, when water quality data were collected.

Sediment Load

The model fit to the measured total suspended sediment (TSS) loads resulted in lower R^2 (0.42) and NSE (0.19) values than for flow, P, and N (Table 7). However, these results were highly dependent on the value observed in December 2010, when approximately $8 \text{ tonTSS month}^{-1}$ were predicted by the model while only $1 \text{ tonTSS month}^{-1}$ was observed in the field data (Figure 5). Without it, the R^2 and NSE values would have reached 0.78 and 0.71, respectively, which would be more in accordance with the results obtained for the N and P.

That difference may be attributable to the quality of field data during that period. In fact, several rain events occurred in December 2010 that produced large flow peaks. The rain event of 19 December 2010 (38 mm) even generated the highest flow peak (Figure 4). Therefore, it was expected that the December 2010 large flow peak would produce a high sediment load as estimated by SWAT. That same trend was observed in March 2011, with SWAT generating high loads consistent with the observed data when heavy rains and high flow peaks also occurred. However, due to the fact that the field data were collected three weeks before the event of 19 December 2010, and after that only in February, the sampled TSS (Total Suspended Solids) concentrations in December 2010 may not be characteristic of that month, meaning that some degree of uncertainty associated to data needs to be taken into account here.

On the other hand, the mismatch between model predictions and field observations in December 2010 may also be attributable to model structure errors. On 19 December 2010, a single rain event carried out 7 of a total of 8 tons of TSS transported during that month. The estimation of this high sediment load on a single day resulted from the high peak runoff rates that the MUSLE equation (Equation (4)) generated. For reduced t_c (higher slopes in the watershed) and high $\alpha_{0.5}$ values, q_{peak} may be several times higher than Q_{surf} , yielding artificial erosion rates.

Similar weaker fits to sediment loads data have been reported in the literature. Dechmi et al. [18] with respect to daily loads (R^2 of 0.18) and Panagopoulos et al. [19] with respect to monthly loads (NSE of 0.34–0.38) linked it to field data extrapolations. Chu et al. [42] with respect to monthly loads (R^2 of 0.19; NSE of 0.11) associated it to possible miss predictions of flow in Warner Creek, Maryland, USA. Aside from the value registered in December 2010, the R^2 (0.78) and NSE (0.71) values obtained are of the same order of magnitude as those of Dechmi et al. [18] for monthly loads (NSE of 0.52–0.72), and Gikas et al. [43] in the Vistonis lagoon, Greece (R^2 generally higher than 0.70 and up to 0.98 in 9 stations). The better fit is also consistent with the fact that the average erosion rates predicted by SWAT in Enxoé in 2010–2011 were similar to the ones measured in the field erosion plots during

that period ($0.1\text{--}0.4\text{ ton ha}^{-1}\text{ year}^{-1}$; Table 7). The erosion plot results are only used for indicative comparison though because data only exist for one year.

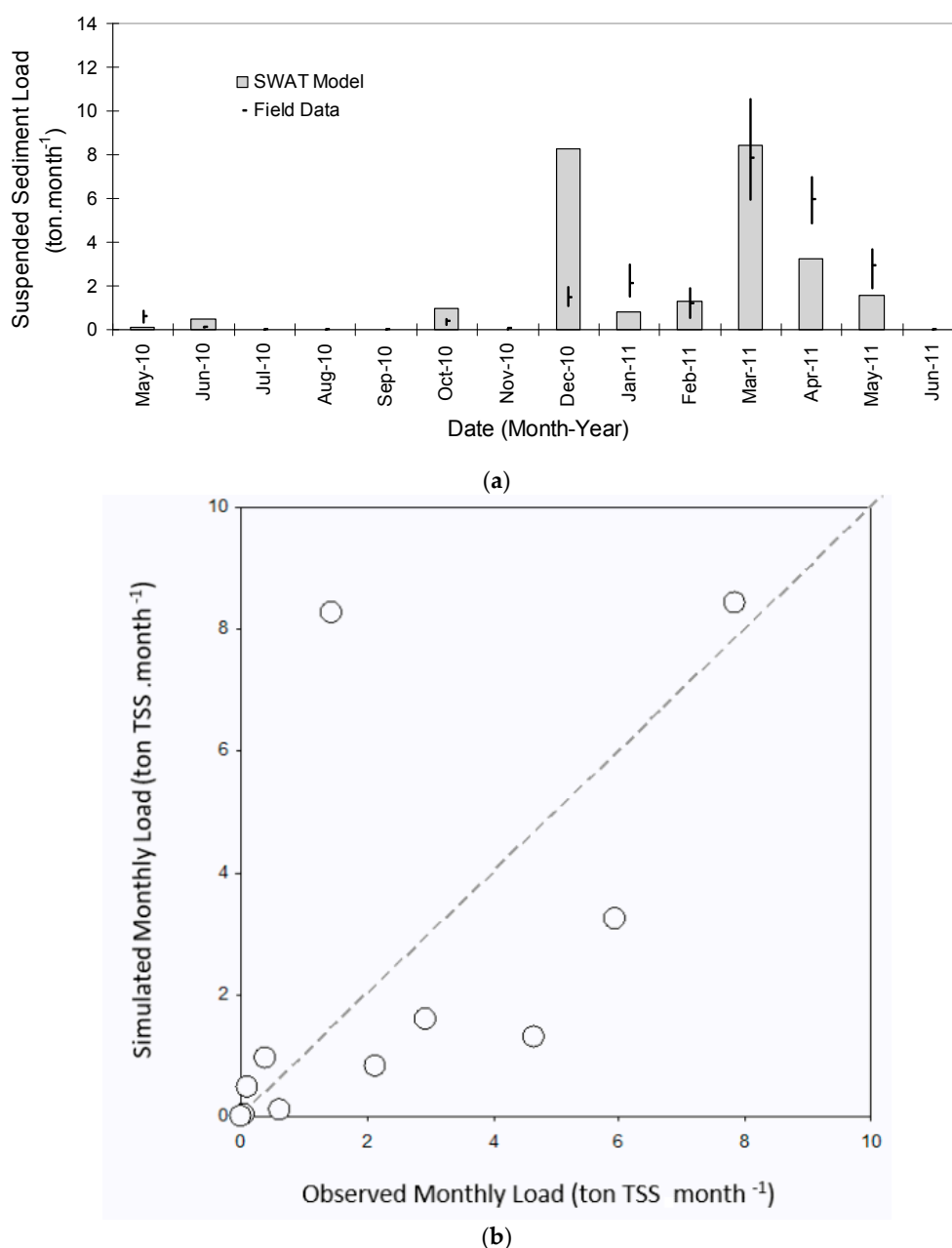
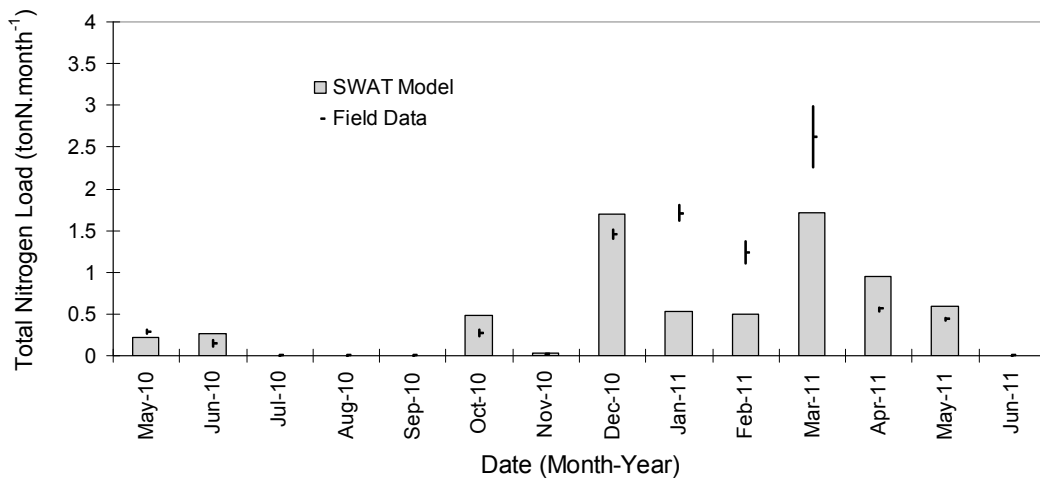


Figure 5. Comparison between the measured and simulated (SWAT) total suspended solids (TSS) loads (a); and scatterplot of the measured versus simulated TSS loads (b) during 2010–2011 (dots denote averages while the segment represents the maximum and minimum monthly load).

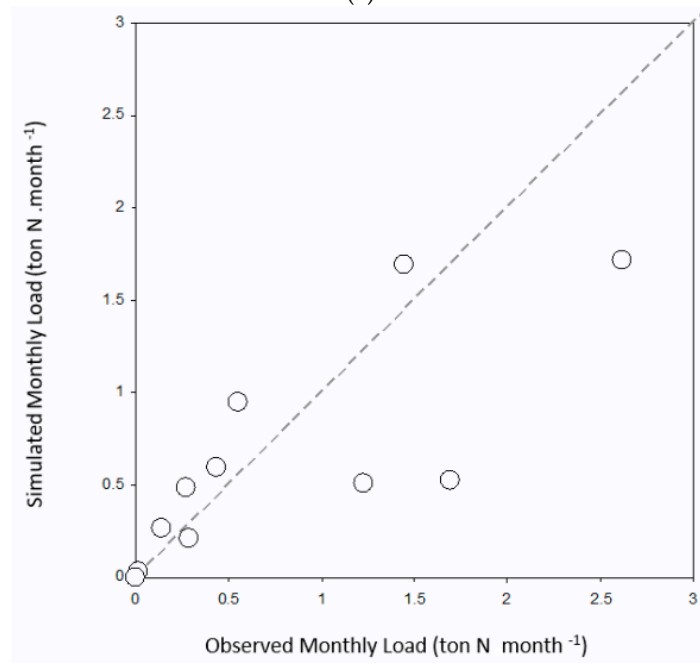
Nutrient Loads

The simulated nutrient loads showed a good fit to the measured field data during 2010–2011. The values of R^2 were relatively high for both N (0.69) and P (0.63), while the NSE values were quite satisfactory (0.65 and 0.62 for N and P, respectively). The RMSE values were also relatively low. These results are in line with reports from other applications using the SWAT model. For example, for the total P monthly load, Dechmi et al. [18] obtained an R^2 of 0.70–0.71 and an NSE of 0.63–0.66, whereas Green and van Griensven [16] obtained higher values for organic P and soluble P (R^2 of 0.72–0.78; NSE of 0.5–0.78), and for nitrate and organic N (R^2 of 0.7–0.8; NSE of 0.68).

The monthly total N (Figure 6) and P (Figure 7) loads showed, as expected, that these were low or nil during the summer months (July to September 2010) when flow was reduced or absent. In the beginning of winter or spring (rainy months) higher loads occurred, with SWAT representing well this trend. However, the model clearly showed an under-prediction of the nutrients loads between January and March 2011, reaching differences of 1 tonN month⁻¹ and 0.05 tonP month⁻¹ when compared to field data. Considering that measured concentrations during these months were fairly stable, the precipitation registered during those months was low (Figure 4), and as a consequence the river flow peaks produced as a direct surface water response were also low, and the visible base flow was still observable because the soil was saturated from the previous months. In these circumstances, model under-predictions of field data during the period between January and March 2011 can only have three possible explanations.

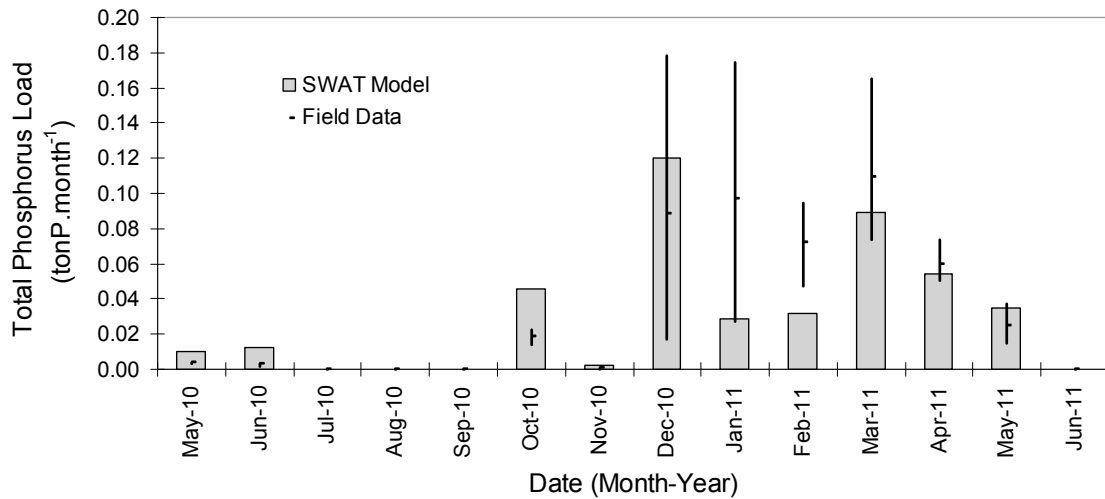


(a)

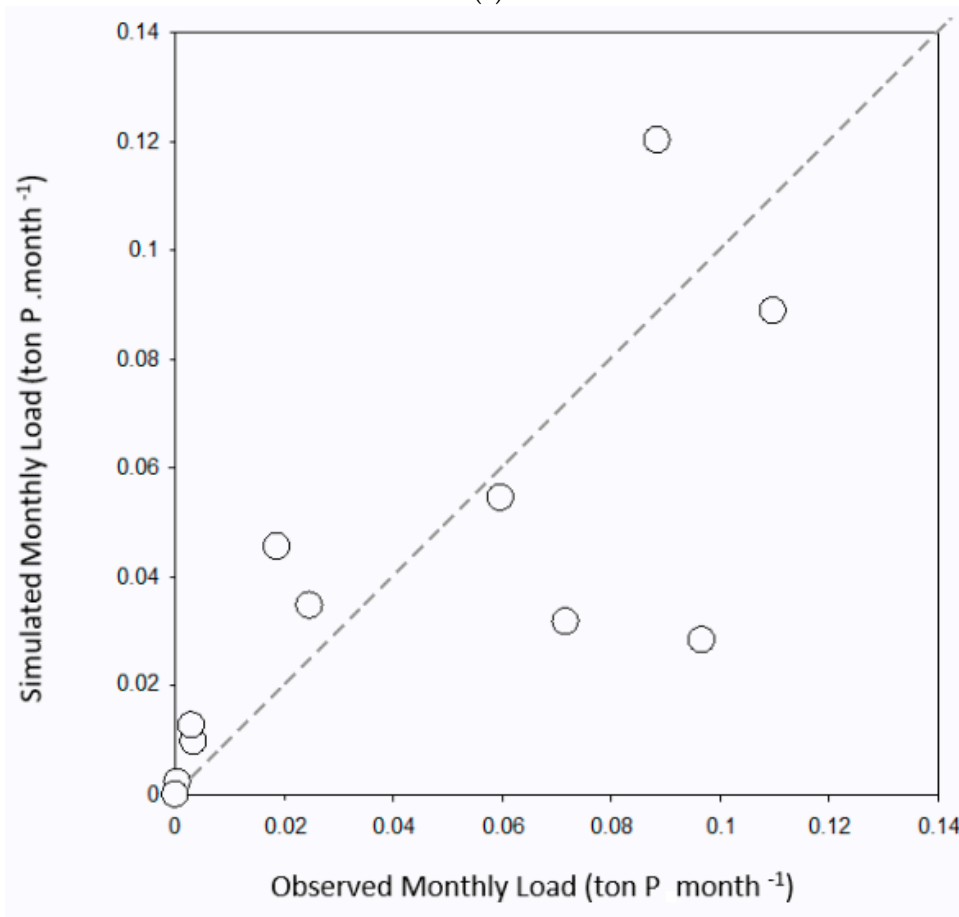


(b)

Figure 6. Comparison between the measured and simulated (SWAT) nitrogen loads (a); and scatterplot of the measured versus simulated nitrogen loads (b) during 2010–2011 (dots denote averages while the segment represents the maximum and minimum monthly load).



(a)



(b)

Figure 7. Comparison between the measured and simulated (SWAT) phosphorus loads (a); and scatterplot of the measured versus simulated phosphorus loads (b) during 2010–2011 (dots denote averages while the segment represents the maximum and minimum monthly load).

Since the surface water flow between January and March 2011 was reduced but the base flow was still present, one could consider that in these months, loads under-predictions could be explained by the lack of groundwater feeding and fertilization. However, this would only affect nitrate transport (P is retained in the surface and is hardly transported through soil or from groundwater to the river). Nevertheless, the SWAT model was tested for the amount of fertilization that would achieve the order

of magnitude of the N loads registered in the field data between January and February 2011. Only by considering an unrealistic high value of 500 kg mineral N ha⁻¹ would it be possible to match those values, as rain, infiltration, percolation, and groundwater flow were not enhanced during these months since, as seen, rain was limited. Furthermore, the vegetation was able to uptake the most part when fertilization amounts were smaller.

A second explanation could be a lack of nutrient loads being delivered by the surface water. However, the surface water was reduced in these months as a result of lower precipitation and flow peaks (Figure 4). Also, TSS loads (transported by surface water) did not exhibit the same under predictive trend as seen for N and P loads. Nonetheless, the type of fertilization (mineral and organic forms) was also tested in SWAT, but the effect was almost unobservable during January and February 2011 due to the low surface water flows; only in the following months was this effect observed, increasing the estimated load and exceeding the field data.

If the explanation for the SWAT under-prediction behavior between January and March 2011 was not found in the surface or groundwater flow, the alternative answer should be the river itself. In SWAT, the in-stream processes are important for defining the order of magnitude of nutrient concentrations in low waters but cannot be used as an infinite source of nutrients. Additionally, the source needed to fit model load predictions to field data in those months would generate abnormal loads in the remaining months. Therefore, the process generating an additional source of nutrients should be mostly present in these months (January to March).

A possible explanation could be related to animal access to the river resulting in a consequent direct nutrient source. However, animals were present in the catchment throughout the year. Moreover, storm events would typically be followed by concentration peaks, specifically of ammonia, that were not verified in field data (ammonia was low, while the concentrations of other N species were stable throughout the seasons).

A more likely explanation should be the development of river beds in the Enxoé river and the biochemical processes that occur at the sediment/water column interface. In Enxoé, the reed bed developed intensively (high density) inside the river sections upstream and downstream of the sampling point where water was retained in pools or shallow aquifers during the spring. These reed beds dried out during the summer and were dragged downstream by high flows in the winter. The remaining roots inside the river bed may have been the organic matter source that promoted in-stream processes mainly after the first winter months, particularly in months with lower flows like January and February 2011, during which the residence time increased (because of the occurrence of disconnected flow and pools). Thus, the reed bed density needed to fit the SWAT loads to field data in those months was quantified. It was assumed percentages of the root fraction of 10–50%, and contents of N of 5–50% and P of 1–10% in those roots (producing a wide range of model results for different crops). A density of 5–10 ton ha⁻¹ in the river bed upstream of the sampling point was determined to be sufficient, which corresponded to 0.5–1 kg biomass m⁻². These amounts are quite reasonable for the Enxoé river because in some areas it is not possible to see the river bed, while in other areas, the occurrence is sparser. In the case of P, the amount needed to develop the reed bed plants (i.e., the amount that may be mineralized in roots and generate the field data loads) was less than the annual deposition load, whereas N could be available from deposition and soil and groundwater nitrate pools. There is little information in the literature about this subject (reed beds are used mostly considered for water treatment) and on the modeling of such in-stream processes. The contributions of these processes do not significantly impact the annual loads (they represent 10 to 20% of the annual load), but because this is an open research subject, these in-stream processes should be studied in more detail in the future, using modeling tools with more advanced stream water quality approaches.

3.2. Enxoé Watershed Long-Term Budget

After model calibration, SWAT was used to understand the catchment dynamics in terms of water and nutrient balance. The computed water, sediment, and nutrient budgets for the thirty-year period

(1980–2010) are presented in Figure 8. Approximately 80–85% of precipitation (annual average is 500 mm) was evapotranspired, while the remaining was transported to the river by groundwater and lateral flow (10–15%) or by runoff (5%).

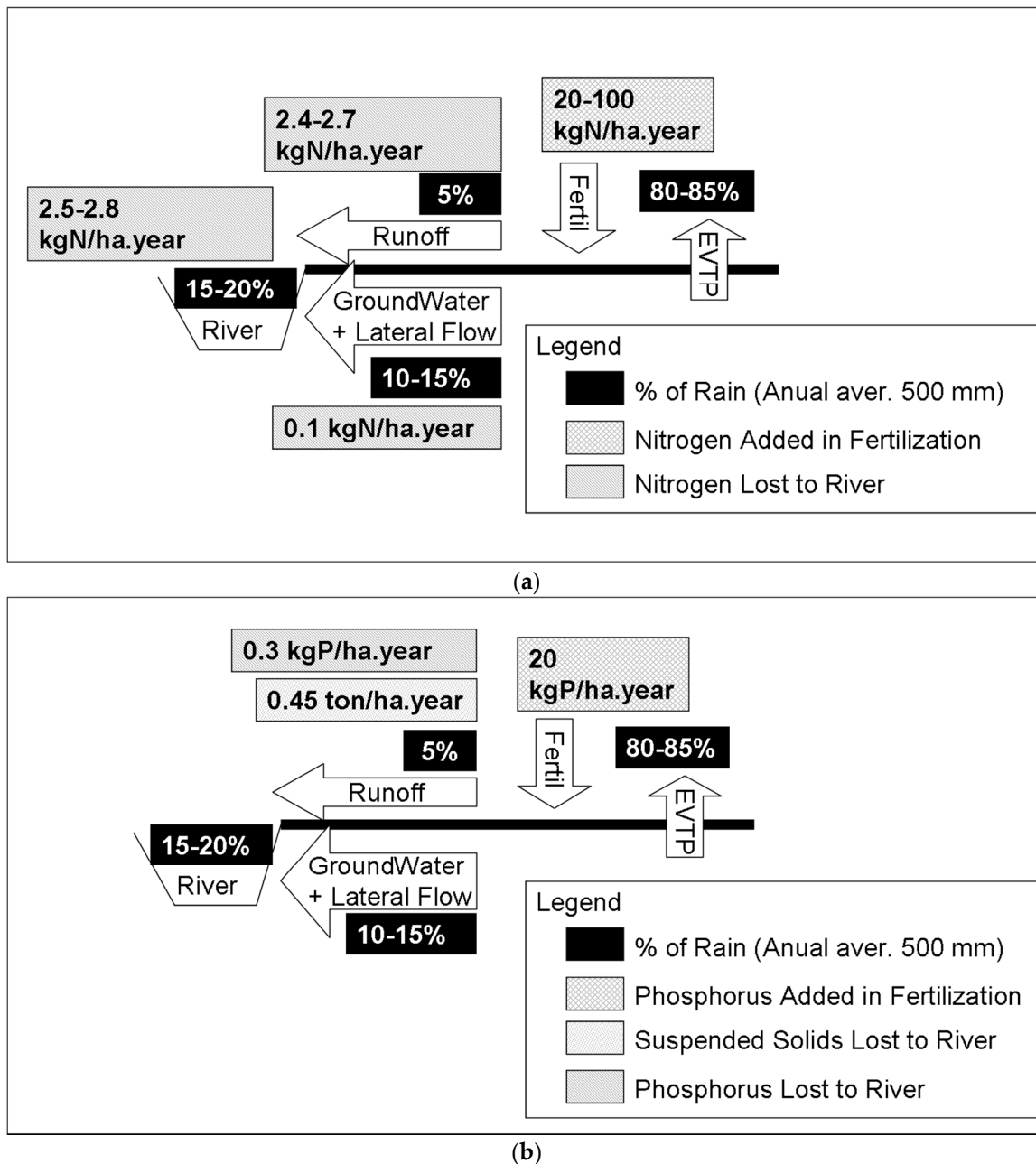


Figure 8. The Enxoé watershed annual average water and nutrient balance and export to the river: water and nitrogen annual averages (a); and sediment and phosphorus annual averages (b).

The annual erosion rate averaged $0.45 \text{ ton ha}^{-1} \text{ year}^{-1}$ (Figure 8) with some sub-basins producing values of up to $1\text{--}2 \text{ ton ha}^{-1} \text{ year}^{-1}$. Kosmas et al. [44] investigated the land use effect on the measured erosion rates in several Mediterranean watersheds and found similar erosion rates in areas cultivated with wheat or olive groves ($0.01\text{--}0.2 \text{ ton ha}^{-1} \text{ year}^{-1}$). Roxo and Casimiro [45] measured values up to $2.5 \text{ ton ha}^{-1} \text{ year}^{-1}$ in erosion plots located in Vale Formoso, Alentejo. Bakker et al. [46] estimated erosion rates of $2\text{--}5 \text{ ton ha}^{-1} \text{ year}^{-1}$ in Amendoeira, a similar sized catchment located in Alentejo, using a soil erosion model. As Enxoé has relatively gentle slopes (2% slope along the river and 5% average slope in the sub-basins) and agriculture is extensive, the simulated/measured erosion rates

can be considered similar to those conducted for sites with similar land uses, slopes, and climate conditions. However, Enxoé erosion rates were considerably low when compared to studies conducted in similar land uses but with higher average slopes. For example, Vanwalleghem [47] reported erosion rates between 29 and 47 ton ha⁻¹ year⁻¹ in three olive groves located in Spain, with average slopes of 25%.

Because of the flushy regime, runoff exports to the river carried 20 times more N (2.4–2.7 kgN ha⁻¹ year⁻¹) than groundwater (0.1 kg ha⁻¹ year⁻¹) (Figure 8). Also, P was mainly transported by runoff because its inorganic forms are normally retained at the soil surface and transported in the particulate form, attached to fine soil particles (erosion). The P export rate was estimated to be 0.3 kg ha⁻¹ year⁻¹ (Figure 8). The nutrient export values in Enxoé were of the same order of magnitude as those obtained by Green and van Griensven [16], who reported values of 1–3 kgN ha⁻¹ year⁻¹ and 0.1–0.3 kgP ha⁻¹ year⁻¹ in small sub-basins with corn and wheat in the USA (annual precipitation was less than 890 mm). Alvarez-Cobelas et al. [48] also reported values of 0.05–7 kgN ha⁻¹ year⁻¹ and 0.0004–1.6 kgP ha⁻¹ year⁻¹ in three semi-arid sub-catchments with vineyards and forest in Spain (annual precipitation was 400 mm). These authors further concluded that high N exports occurred in areas where agriculture was more nutrient intensive and the annual precipitation was higher, promoting nitrate leaching. For example, Salvia-Castellví et al. [49] found nitrate exports of 27–33 kgN ha⁻¹ year⁻¹ in agricultural watersheds with annual precipitation ranging from 700–1200 mm. On the other end, P exports tend to be higher in areas with high erosion and can reach hundreds of kgP ha⁻¹ in a single event, as described in Ramos and Martínez-Casasnovas [50,51] for a vineyard in northeast Spain.

Based on SWAT simulations (30 years), the nutrient loads delivered to the Enxoé reservoir were estimated to be 18 tonN year⁻¹ and 0.7 tonP year⁻¹, which can be considered within the same range as those obtained in other extensive agricultural areas with gentle slopes (low erosion) and reduced human presence. SWAT simulations further showed that 90% of the annual N and P loads was delivered, on average, to the reservoir over 15 days, while 90% of the sediment load was delivered over 8 days (Table 8). This behavior, where high concentrations are transported in short time periods, is an important feature in temporary flushy regimes and may have a significant impact on the reservoir [52]. Thus, future work will involve the application of a reservoir model that will be fed by the loads estimated in this study in order to test different management strategies to reduce the trophic state of the Enxoé reservoir.

Table 8. Number of days to achieve 90% of the annual load transported to the Enxoé reservoir (SWAT average predictions for the period 1980–2010).

	N of Days to Transport 90% of Annual Load		
	Total N	Total P	TSS
Average	12	14	8
Maximum	28	27	23
Minimum	1	1	1

4. Conclusions

This study aimed at understanding the water and nutrient long-term dynamics in the Enxoé catchment, and quantifying nutrient loads to the Enxoé reservoir. SWAT model predictions of the monthly flow, and sediment, P, and N loads were compared to the field data, producing R² values between 0.42–0.78, and NSE value between 0.19–0.77. The SWAT model was thus able to capture the main long-term trends and processes that generate, transport, and transform nutrients in the Enxoé watershed.

Model simulations showed that the Enxoé River is characterized by a temporary flushy regime where high concentrations are transported in short time periods. N (2.5–2.8 kg ha⁻¹ year⁻¹), suspended solids (0.45 ton ha⁻¹ year⁻¹), and P (0.3 kg ha⁻¹ year⁻¹) exports reach the reservoir mainly by runoff and over a very short number of days (8–15 days). As a result, nutrient loads delivered to the Enxoé

reservoir were estimated to be 18 tonN year⁻¹ and 0.7 tonP year⁻¹ (30-year simulation). These results can be considered within the same range as those obtained in other extensive agricultural areas with gentle slopes (low erosion) and reduced human presence.

The average to low nutrient inputs from the watershed suggest that the high eutrophic status of the reservoir may not be due only to the input loads. The reservoir geometry (average depth of 5 m) may also promote high light availability at the bottom where nutrient and organic matter accumulate from watershed floods, deposition, and diagenesis. Nutrient release to the water column may then support the phytoplankton communities. This hypothesis will be tested by integrating SWAT results into a reservoir model to depict the origin of the Enxoé trophic status and test management scenarios that may reduce it.

Because Enxoé is a small temporary watershed with a tendency toward a flushy regime, and in-stream processes may have an important role on describing the nutrient concentrations in low waters, two parallel research topics are suggested for future investigation: i) The role of floods on watershed dynamics and on annual loads; and ii) the analysis of in-stream and pool water quality processes occurring in low waters and discontinued flow.

Author Contributions: D.B. ran model simulations and wrote the paper; M.A.B., A.P. and S.R. performed the laboratory analysis; M.C.G., R.N., and T.B.R. revised a first draft version of this paper.

Funding: The present work was supported within the framework of the EU Interreg SUDOE IVB program (SOE1/P2/F146 AguaFlash project), the Project Mirage (EU-FP7), and the Project EUTROPHOS (PTDC/AGR-AAM/098100/2008) of the Fundação para a Ciência e a Tecnologia (FCT). MATEREC acknowledges funding from FCT/MCTES (PIDDAC) through project UID/EEA/50009/2019. T. B. Ramos was supported by the FCT grant SFRH/BPD/110655/2015.

Conflicts of Interest: The authors declare no conflict of interest.

References

1. CCDR Alentejo. *Anuário de recursos hídricos do Alentejo. Ano Hidrológico 2003/2004*; MAOTDR: Évora, Portugal, 2005. (In Portuguese)
2. Instituto Nacional da Água. *Poluição Provocada por Nitratos de Origem Agrícola. Directiva 91/676/CEE, de 12 de Dezembro de 1991. Relatório (2004–2007)*; Publicação conjunta do MAOTDR e MADRP: Lisboa, Portugal, 2008. (In Portuguese)
3. Instituto Nacional da Água. *Management of the Trophic Status in Portuguese Reservoirs Volume I Criteria and Assessment of the Trophic Status. Study in the Scope of WWTP Directive and Sensitive Area Plans*; Instituto Nacional da Água: Lisboa, Portugal, December 2009.
4. Instituto Nacional da Água. *Plano de Ordenamento da Albufeira do Enxoé, Estudos de Caracterização e Pré-Proposta de Ordenamento*; Instituto da Água, MAOTDR: Lisboa, Portugal, 2004. (In Portuguese)
5. Valério, E.; Pereira, P.; Saker, M.L.; Franca, S.; Tenreiro, R. Molecular characterization of *Cylindrospermopsis raciborskii* strains isolated from Portuguese freshwaters. *Harmful Algae* **2005**, *4*, 1044–1052. [[CrossRef](#)]
6. Paerl, H.W.; Fulton, R.S.; Moisander, P.H.; Dyble, J. Harmful freshwater algal blooms: With an emphasis on cyanobacteria. *Sci. World J.* **2001**, *1*, 76–113. [[CrossRef](#)] [[PubMed](#)]
7. Havens, K.E.; James, R.T.; East, T.L.; Smith, V.H. N:P ratios, light limitation, and cyanobacterial dominance in a subtropical lake impacted by non-point source nutrient pollution. *Environ. Poll.* **2003**, *122*, 379–390. [[CrossRef](#)]
8. Rolff, C.; Almesjo, L.; Elmgren, R. Nitrogen fixation and abundance of the diazotrophic cyanobacterium *Aphanizomenon* sp. in the Baltic Proper. *Mar. Ecol. Prog. Ser.* **2007**, *332*, 107–118. [[CrossRef](#)]
9. Coelho, H.; Silva, A.; Chambel-Leitão, P.; Obermann, M. On the origin of cyanobacteria blooms in the Enxoé reservoir. In Proceedings of the 13th World Water Congress, International Water Resources Association, Montpellier, France, 1–4 September 2008.
10. Ramos, T.B.; Gonçalves, M.C.; Branco, M.A.; Brito, D.; Rodrigues, S.; Sánchez-Pérez, J.M.; Suavage, S.; Prazeres, A.; Martins, J.C.; Fernandes, M.L.; et al. Sediment and nutrient dynamics during storm events in the Enxoé temporary river, southern Portugal. *Catena* **2015**, *127*, 177–190. [[CrossRef](#)]

11. Ramos, T.B.; Rodrigues, S.; Branco, M.A.; Prazeres, A.; Brito, D.; Gonçalves, M.C.; Martins, J.C.; Fernandes, M.L.; Pires, F.P. Temporal variability of soil organic carbon transport in the Enxóe agricultural watershed. *Environ. Earth Sci.* **2015**, *73*, 6663–6676. [[CrossRef](#)]
12. Neitsch, S.L.; Arnold, J.G.; Kiniry, J.R.; Williams, J.R. *Soil and Water Assessment Tool, Theoretical Documentation, Version 2009*; Technical Report, No. 406; Texas Water Resources Institute: College Station, TX, USA, 2011.
13. Gassman, P.W.; Reyes, M.R.; Green, C.H.; Arnold, J.G. The Soil and Water Assessment Tool: Historical development, applications, and future research directions. *Trans. ASABE* **2007**, *50*, 1211–1250. [[CrossRef](#)]
14. Zhang, X.; Srinivasan, R.; Van Liew, M. Multi-Site Calibration of the SWAT Model for Hydrologic Modeling. *Trans. ASABE* **2008**, *51*, 2039–2049. [[CrossRef](#)]
15. Geza, M.; McCray, J.E. Effects of soil data resolution on SWAT model stream flow and water quality predictions. *J. Environ. Manag.* **2008**, *88*, 393–406. [[CrossRef](#)] [[PubMed](#)]
16. Green, C.H.; van Griensven, A. Autocalibration in hydrologic modeling: Using SWAT2005 in small-scale watersheds. *Environ. Model. Softw.* **2008**, *23*, 422–434. [[CrossRef](#)]
17. Yevenes, M.A.; Mannaerts, C.M. Seasonal and land use impacts on the nitrate budget and export of a mesoscale catchment in Southern Portugal. *Agric. Water Manag.* **2011**, *102*, 54–65. [[CrossRef](#)]
18. Dechmi, F.; Burguete, J.; Skhiri, A. SWAT application in intensive irrigation systems: Model modification, calibration and validation. *J. Hydrol.* **2012**, *470–471*, 227–238. [[CrossRef](#)]
19. Panagopoulos, Y.; Makropoulos, C.; Mimikou, M. Reducing surface water pollution through the assessment of the cost-effectiveness of BMPs at different spatial scales. *J. Environ. Manag.* **2011**, *92*, 2823–2835. [[CrossRef](#)]
20. Debele, B.; Srinivasan, R.; Parlange, J.-Y. Coupling upland watershed and downstream waterbody hydrodynamic and water quality models (SWAT and CE-QUAL-W2) for better water resources management in complex river basins. *Environ. Model. Assess.* **2008**, *13*, 135–153. [[CrossRef](#)]
21. Brito, D.; Neves, R.; Branco, M.C.; Gonçalves, M.C.; Ramos, T.B. Modeling flood dynamics in a temporary river draining to an eutrophic reservoir in southeast Portugal. *Environ. Earth Sci.* **2017**, *76*, 377. [[CrossRef](#)]
22. Brito, D.; Ramos, T.B.; Gonçalves, M.C.; Morais, M.; Neves, R. Integrated modelling for water quality management in a eutrophic reservoir in south-eastern Portugal. *Environ. Earth Sci.* **2018**, *77*, 40. [[CrossRef](#)]
23. Ramos, T.B.; Darouich, H.; Gonçalves, M.C.; Brito, D.; Castelo Branco, M.A.; Martins, J.C.; Fernandes, M.L.; Pires, F.P.; Morais, M.; Neves, R. An integrated analysis of the eutrophication process in the Enxóe reservoir within the DPSIR framework. *Water* **2018**, *10*, 1576. [[CrossRef](#)]
24. Census. *Recenseamento Geral Agrícola*; Instituto Nacional de Estatística: Lisboa, Portugal, 2001.
25. European Environmental Agency. Corine Land Cover. Available online: <https://www.eea.europa.eu/publications/COR0-landcover> (accessed on 30 November 2017).
26. Ritchie, J.T. Model for predicting evaporation from a row crop with incomplete cover. *Water Resour. Res.* **1972**, *8*, 1204–1213. [[CrossRef](#)]
27. Jensen, M.E.; Burman, R.D.; Allen, R.G. *Evapotranspiration and Irrigation Water Requirements*; ASCE Manuals and Reports on Engineering Practice No. 70; ASCE: New York, NY, USA, 1990; 332p.
28. USDA-SCS. Section 4: Hydrology. In *National Engineering Handbook*; Natural Resources Conservation Service: Washington, DC, USA, 1972.
29. William, J.R. Sediment routing for agricultural watersheds. *Water Resour. Bull.* **1975**, *11*, 965–974. [[CrossRef](#)]
30. Wischmeier, W.H.; Smith, D.D. *Predicting Rainfall Erosion Losses: A Guide to Conservation Planning*; Agriculture Handbook 282; USDA-ARS: Washington, DC, USA, 1978.
31. McElroy, A.D.; Chiu, S.Y.; Nebgen, J.W.; Aleti, A.; Bennet, F.W. Loading Functions for Assessment of Water Pollution from Nonpoint Sources. Environmental Protection Technology Series; EPA 600/2-76-151; EPA: Washington, DC, USA, 1976.
32. Williams, J.R.; Hann, R.W. *Optimal Operation of Large Agricultural Watersheds with Water Quality Constraints*; Texas Water Resources Institute, Texas A&M Univ. Tech. Rep. No. 96; Texas Water Resources Institute: College Station, TX, USA, 1978.
33. Serviço Nacional de Informação dos Recursos Hídricos. Available online: <http://snirh.apambiente.pt/> (accessed on 30 November 2017).
34. Ministry of Agriculture. *Código das Boas Práticas Agrícolas Para a Protecção da Água Contra a Poluição de Nitratos de Origem Agrícola*; MADRP: Lisboa, Portugal, 1997. (In Portuguese)

35. Galván, L.; Olías, M.; Fernandez de Villarán, R.; Domingo Santos, J.M.; Nieto, J.M.; Sarmiento, A.M.; Cánovas, C.R. Application of the SWAT model to an AMD-affected river (Meca River, SW Spain). Estimation of transported pollutant load. *J. Hydrol.* **2009**, *377*, 445–454. [[CrossRef](#)]
36. Perrin, J.; Ferrant, S.; Massuel, S.; Dewandel, B.; Maréchal, J.C.; Aulong, S.; Ahmed, S. Assessing water availability in a semi-arid watershed of southern India using a semi-distributed model. *J. Hydrol.* **2012**, *460–461*, 143–155. [[CrossRef](#)]
37. Brown, L.C.; Barnwell, T.O., Jr. *The Enhanced Water Quality Models QUAL2E and QUAL2E-UNCAS Documentation and User Manual*; EPA Document EPA/600/3-87/007; USEPA: Athens, GA, USA, 1987.
38. Nash, J.E.; Sutcliffe, J.V. River flow forecasting through conceptual models: Part 1. A discussion of principles. *J. Hydrol.* **1970**, *10*, 282–290. [[CrossRef](#)]
39. Moriasi, D.N.; Arnold, J.G.; Van Liew, M.W.; Bingner, R.L.; Harmel, R.D.; Veith, T.L. Model evaluation guidelines for systematic quantification of accuracy in watershed simulations. *Trans. ASABE* **2007**, *50*, 885–900. [[CrossRef](#)]
40. Fohrer, N.; Eckhardt, K.; Haverkamp, S.; Frede, H.G. Applying the SWAT Model as a Decision Support Tool for Land Use Concepts in Peripheral Regions in Germany. In *Sustaining the Global Farm, Selected Papers from the 10th International Soil Conservation Organization Meeting*; Stott, D.E., Mohtar, R.H., Steinhardt, G.C., Eds.; Purdue: West Lafayette, IN, USA, 2001; pp. 994–999.
41. Lillebø, A.I.; Morais, M.; Guilherme, P.; Fonseca, R.; Serafim, A.; Neves, R. Nutrient dynamics in Mediterranean temporary streams: A case study in Pardielas catchment (Degebe River, Portugal). *Limnologica* **2007**, *37*, 337–348. [[CrossRef](#)]
42. Chu, T.W.; Shirmohammadi, A.; Montas, H.; Sadeghi, A. Evaluation of the SWAT model's and nutrient components in the piedmont physiographic region of Maryland. *Trans. ASAE* **2004**, *47*, 1523–1538. [[CrossRef](#)]
43. Gikas, G.D.; Yiannakopoulou, T.; Tsihrintzis, V.A. Modeling of nonpoint-source pollution in a Mediterranean drainage basin. *Environ. Model. Assess.* **2005**, *11*, 219–233. [[CrossRef](#)]
44. Kosmas, C.; Danalatos, N.; Cammeraat, L.H.; Chabart, M.; Diamantopoulos, J.; Farand, R.; Gutierrez, L.; Jacob, A.; Marques, H.; Martinez-Fernandez, J.; et al. The effect of land use on runoff and soil erosion rates under Mediterranean conditions. *Catena* **1997**, *29*, 45–59. [[CrossRef](#)]
45. Roxo, M.J.; Casimiro, P.C. Long Term Monitoring of Soil Erosion by Water, Vale Formoso Erosion Centre—Portugal'. Soil Conservation and Protection for Europe Project. Available online: http://eussoils.jrc.ec.europa.eu/projects/scape/uploads/97/Roxo_Casimiro.pdf (accessed on 12 August 2016).
46. Bakker, M.M.; Govers, G.; van Doorn, A.; Quetier, F.; Chouvardas, D.; Rounsevell, M. The response of soil erosion and sediment export to land-use change in four areas of Europe: The importance of landscape pattern. *Geomorphology* **2008**, *98*, 213–226. [[CrossRef](#)]
47. Vanwalleghe, T.; Amate, J.I.; de Molina, M.G.; Fernández, D.S.; Gómez, J.A. Quantifying the effect of historical soil management on soil erosion rates in Mediterranean olive orchards. *Agric. Ecosyst. Environ.* **2011**, *142*, 341–351. [[CrossRef](#)]
48. Alvarez-Cobelas, M.; Sánchez-Andrés, R.; Sánchez-Carrillo, S.; Angeler, D.G. Nutrient contents and export from streams in semiarid catchments of central Spain. *J. Arid Environ.* **2010**, *74*, 933–945. [[CrossRef](#)]
49. Salvia-Castellví, M.; Iffly, J.F.; Borght, P.V.; Hoffmann, L. Dissolved and particulate nutrient export from rural catchments: A case study from Luxembourg. *Sci. Total Environ.* **2005**, *344*, 51–65. [[CrossRef](#)] [[PubMed](#)]
50. Ramos, M.C.; Martínez-Casasnovas, J.A. Nutrient losses from a vineyard soil in Northeastern Spain caused by an extraordinary rainfall event. *Catena* **2004**, *55*, 79–90. [[CrossRef](#)]
51. Ramos, M.C.; Martínez-Casasnovas, J.A. Nutrient losses by runoff in vineyards of the Mediterranean Alt Penedès region (NE Spain). *Agric. Ecosyst. Environ.* **2006**, *113*, 356–363. [[CrossRef](#)]
52. González-Hidalgo, J.C.; Peña-Monné, J.L.; de Luis, M. A review of daily soil erosion in Western Mediterranean areas. *Catena* **2007**, *71*, 193–199. [[CrossRef](#)]

